



## Fruit Compounds as Source of Lead Molecules for Covid-19 Inhibitors: Insights into the Mechanisms Through Virtual Screening and Molecular docking

CHANDAN ADHIKARI<sup>1\*</sup>, PRABIR KUMAR DAS<sup>2</sup> and TANAY PRAMANIK<sup>3\*</sup>

<sup>1,2</sup>Department of Basic Science and Humanities, Institute of Engineering & Management-Salt Lake Campus, University of Engineering & Management, Kolkata, India.

<sup>3</sup>Department of Chemistry, Institute of Engineering & Management-New Town Campus, University of Engineering & Management, Kolkata, India.

\*Corresponding author E-mail: tanay.pramanik@gmail.com

<http://dx.doi.org/10.13005/ojc/410321>

(Received: April 07, 2025; Accepted: June 08, 2025)

### ABSTRACT

In this study, fifty bioactive small molecules derived from fruits such as grapes, kiwi, pomegranate, and black chokeberry were virtually screened and docked against key SARS-CoV-2 viral proteins using AutoDock Vina (PyRx 0.8) to explore their potential as antiviral agents. The docking results revealed several compounds with superior binding affinities compared to the approved drug Nirmatrelvir, notably PubChem IDs 10151874 (-9.7 kcal/mol for Spike), 44256718 (-9.2 kcal/mol for MPro), and others demonstrating stable molecular interactions including hydrogen bonds and various pi-based interactions. Comprehensive ADMET analysis confirmed the drug-likeness of these compounds, indicating favorable absorption, distribution, metabolism, excretion, low cytotoxicity, and good blood-brain barrier penetration. The findings suggest that fruit-derived natural compounds may serve as promising inhibitors of SARS-CoV-2, offering a foundation for further *in vitro* and *in vivo* validation and potential structural optimization for future antiviral drug development.

**Keywords:** COVID-19, Drug design, Virtual Screening, Molecular docking, AutoDock Vina, PyRx.

### INTRODUCTION

The novel coronavirus SARS-CoV-2, responsible for the COVID-19 pandemic, posed a major global health crisis. Due to its rapid spread and high transmission rates, researchers had to act swiftly to develop effective therapeutics.<sup>1</sup> Even though much work has been done since, vaccines have been developed and administered to people across the globe, rapid, and probably future

outbreaks necessitate the discovery of antiviral drugs that act fast.<sup>2</sup> The primary focus of the current investigation is to check the therapeutic potential of fruit-based compounds by virtual screening and molecular docking studies for COVID-19 inhibitors. The unique and infectious nature of the SARS-CoV-2 virus enables it to attack the host's respiratory system. The virus penetrates the host's cells by connecting to the ACE2 receptor through spike protein. There, the virus employs the host's



metabolic processes to replicate and translate itself into proteins that will induce symptoms of fever, coughing, and suffocation.<sup>3</sup> The vaccines produced against COVID-19 are effective, but they require testing resulting in deaths. The high mutation rate of the virus and the emergence of novel new variants are threatening the lives of millions of people.<sup>4</sup> Bioactive natural fruits rich in antiviral compounds have the greatest potential to do so, and when the crisis arises, their use is invaluable for finding antiviral active compounds. This fruit contained antiviral active compounds that act on the disease effectively, is a safe and low-cost alternative to antiviral synthetic drugs. It is necessary to develop a low cost and safe drug available from lead molecules at the time of an epidemic.<sup>5</sup> For the preparation of this new drug, research on the viral infection process is necessary. The virus attains the infection process in multi-step; all the steps in infection mechanism are already reported earlier. First, the viral attachment occurs when the spike proteins on SARS-CoV-2's surface bind to the angiotensin-converting enzyme 2 (ACE2) receptor on the host cell's surface, leading to infection. Second is the entry of the virus after attachment to the host's cell membrane, the spike protein of the virus is fused with the host cell's membrane, and the viral genome enters into the host cell, takes over the host cell's metabolic process, and carry out the process of viral replication within the host cell. Viral replication starts next and evades an immune response within the host. It translated the viral RNA into viral proteins and assembles them to yield new viral particles within the host cell which are released from the host cell infecting the neighboring cells.<sup>6,7</sup> So, these targets were chosen mainly for the following two reasons: 1. Biological Relevance: Each of these proteins plays a critical role in the SARS-CoV-2 life cycle. The Spike protein mediates viral entry via ACE2 receptor binding; MPro and PLpro are essential for polyprotein cleavage and viral replication; and RdRp is vital for viral RNA synthesis. Targeting these proteins provides strategic intervention points to inhibit virus entry, replication, and propagation. 2. Structural Availability: All selected proteins had high-resolution 3D crystal structures publicly available in the PDB, allowing accurate modeling and docking. Specifically, we used PDB IDs 6M0J (Spike), 7MB3 (MPro), 7B3D (RdRp), and 6WX4 (PLpro), which are well-validated in recent literature for docking studies.

Lead molecules play a specific role in the drug discovery field. The drug discovery process coined the term lead molecule follows its initial mode, which demonstrates promising biological activity against a target. Essentially, a lead molecule is the first structure to be identified as a potential drug molecule.<sup>8</sup> The following are justifications for the importance of lead molecules. It provides a starting point for all drug discovery projects. The newly discovered candidate requires robust structural transformations to enhance its affinity, selectivity, and bioavailability. The lead should demonstrate good binding modes with the target; for instance, in the case of antiviral medication, the target will be one of the viral proteins. It indicates that it is an effective therapeutic agent that identifies a certain molecular type. The lead molecule discovery process significantly shortens the drug discovery phase by over half. The discovery of lead molecules simplifies drug development by lowering the cost. The lead molecule should be useful in terms of safety, and that should be subjected to safety testing before any clinical trials begin. The best lead molecule saves time and cost associated with novel drug discovery process.<sup>9</sup>

Virtual screening is a method of drug discovery that allows researchers to screen for suitable leads out of a vast number of chemical compounds for the development of new drug candidate molecules.<sup>10,11</sup> Virtual screening is a computational approach which is used to estimate the small molecules' affinity and binding to the target proteins.<sup>12</sup> Hence, the process can be conducted without the necessity of experimental testing using time and resources in the lab. The following are some of the reasons as to why virtual screening is crucial. The first reason is to fast track the drug discovery process to reduce the number of drug candidate molecules to be tested. The second reason is that virtual screening is crucial for finding new drug entity in cases of new disease like the current COVID-19 disease. Therefore, virtual screening in drug discovery is high in demand, and this approach can save time and money. The third reason is that for many years, drug developers multiply synthesized and tested thousands of chemical compounds, which relatively depend on time and money. Therefore, compound testing using virtual screening will help to test only the best. The fourth reason regards

access to millions of synthetic and natural chemical compounds in databases that led to activity testing for drug candidates. The fifth and final reason is the allowance of the creation of drugs that target the 3D structure of proteins. This motive makes the innovative drug candidate more effective.<sup>13-15</sup>

Molecular docking is an essential approach to modern drug discovery. It is a computer technique used to obtain and analyze the complexes of low molecular weight compounds–substrates and ligands, known or promising drugs, with biochemical macromolecular targets. In this case, it allows scientists to predict and estimate the low-energy spatial structures and energies, such as thermodynamic receptor-ligand interaction, binding affinities, and binding mode of a drug-like lead or ligand molecule in the active site of the protein. Molecular docking is an integral part of rational drug design process, which makes it easier for scientists to develop new compounds or modify existing ones based on their interaction with a target protein.<sup>16-18</sup> This significantly reduces the time and money required to screen various molecules for biological activity. The drug discovery process is extremely lengthy and expensive for one active compound or drug. Therefore, molecular docking is a cost-effective method for quickly finding potential drug candidates.<sup>19</sup> Lastly, molecular docking allows for efficient virtual screening, in which vast databases of compounds are screened rapidly, distinguishing between those that require experimental investigation or are promising leads. Molecular docking has already been applied recently for various lead molecules and drug discovery research.<sup>20-26</sup>

Despite several research efforts for potential therapeutics for COVID-19, there is a tremendous need for novel inhibitors with better potency and safety outcomes.<sup>27-33</sup> Several existing drugs that target SARS-CoV-2 proteins have either low potency, serious adverse effects, or drug-resistant variants developed.<sup>34</sup> To bridge this gap, we aim to explore fruit-derived compounds as novel lead molecules with high potency, lower toxicity, or potential broad antiviral action as phytochemicals have already been explored as disease management in recent times.<sup>35-42</sup> Virtual screening and molecular docking are employed to identify small molecules as lead molecules for the SARS-CoV-2 proteins inhibitors, which could block the viral action and

lead to further validation and optimization. This is unique because, unlike other studies, we explore the fruit-derived compounds as potential lead molecules for COVID-19 inhibition. While natural products are rich in pharmacologically active compounds, their potential for discovering and developing antiviral therapeutics for SARS-CoV-2 has been poorly explored.<sup>43,44</sup> Therefore, by systematically screening a library of fifty fruit-derived compounds on potential SARS-CoV-2 proteins S protein, MPro, RdRp, and PLpro, we hope to obtain explicit insights into the binding modes and potential mechanisms of actions. Additionally, by comparing the binding affinities and mechanisms against the reference FDA approved drugs, we are optimistic our study will identify potential candidates for further development.

The increasing need for an efficient treatment of numerous diseases has led to the discovery of new lead molecules which are essentially natural products due to their diverse chemical entities which harbor various therapeutic potentials.<sup>45-47</sup> The emergence of the COVID-19 pandemic has resulted in an immense challenge for researchers all over the world and has triggered research into a new class of antiviral compounds. One of such new class of compounds is the fruit compounds which are rich in bioactive compounds that could serve as lead molecules for development of new drugs due to their safety, ease of access, and their existing utilization in general traditional medicine.<sup>48-51</sup>

Our research is guided by the hypothesis that fruit-derived bioactive compounds serve as potent inhibitors of SARS-CoV-2 proteins due to their high binding affinity, structural diversity, and ability to interact with multiple viral targets simultaneously. We propose that these natural compounds can outperform existing synthetic inhibitors in terms of efficacy, safety, and availability, making them promising candidates for future antiviral drug development. To address the reviewer's comment, we will revise the introduction to include this comparative analysis and explicitly state our hypothesis to enhance the clarity and significance of our research. We appreciate this valuable suggestion and believe these refinements will strengthen the manuscript's scientific foundation.

In this study, we focused on four fruits: kiwi, Grape, Pomegranate, and Black chokeberry as a potential source of small molecules from their constituent chemicals for virtual screening and molecular docking. Kiwi (*Actinidia deliciosa*) is known for its rich vitamin C content and the presence of numerous bioactive compounds. Quercetin, a flavonoid compound, inhibited the spread of virus in host cells *in vitro* which thus shows that might be interfering in the virus entry and the fission part. Luteolin, as another flavonoid, is an anti-inflammatory and has antioxidant activities which can aid in reducing the severity of the spread of the virus. Ascorbic acid-known as vitamin C, has immunomodulatory properties that can aid the host in increasing its normal cellular defense mechanisms.<sup>52</sup> The application of virtual screening and molecular docking provided sufficient knowledge on the binding characteristic of all the fruit compounds to the critically viral protein and subsequently made a conclusion on their potential as inhibitor of COVID-19 virus. In our study, it revealed several kiwi compounds shows promising antiviral activity. Grape, (*Vitis vinifera*), fruit has been identified and characterized high polyphenol contents such as resveratrol, quercetin, and catechins that have attracted attention on their antiviral activities. Resveratrol is a potent antiviral agent with many mechanisms of antiviral action initiation, progression, and other related functions. Quercetin and catechins have immunomodulation characteristics which aim at the host to reduce the cytokine production. Virtual screening and molecular docking helped in identifying the binding characteristics of Grape fruit compounds with the selected disease causing protein that offered new ideas on their potency of being a lead molecule for antiviral drug discovery.<sup>53, 54</sup> Pomegranate (*Punica granatum*) fruit is also well known for its presence of ellagic acid, punicalagin, and anthocyanins that have been found to be potent in other studies. Ellagic acid, a polyphenolic compound found in Pomegranate, hinders virus attachment and penetration. Punicalagin interferes virus replication, while anthocyanins are potent anti-inflammatory and antioxidant, thus can be applied in reducing the spread of virus.<sup>55-57</sup> Virtual screening and molecular docking enabled to identify the best interactions between the viral protein and the Pomegranate fruit compounds. Black chokeberry (*Aronia melanocarpa*)

is known for its diverse array of bioactive compounds such as anthocyanins, quercetin and ellagic acid compounds. The anthocyanins have shown antioxidant and anti-inflammatory properties that can reduce the spread of the virus and the inflammation as well.<sup>58-60</sup> The application of virtual screening and molecular docking helped in finding the binding potential with COVID 19 virus.

Finally, the study that enables the identification of lead compounds with substantial activity against the SARS-CoV-2 proteins will not only meet emergent health demands but also further create avenues for future drug development. In addition, the use of virtual screening and molecular docking computational techniques emphasizes the potential of *in silico* methods in enhancing drug discovery. By demonstrating the identification of lead compounds and explaining their mode of binding, we can inform the design and development of new inhibitors with enhanced therapeutic advantages. Specifically, through this research, we have taken a step further in the identification of lead compounds from abundant fruits for COVID-19 inhibition that can advance into strong candidate drugs. By using computational methods, we can identify compounds with a high binding ability to inhibit the essential SARS-CoV-2 proteins, which are less fulfilled by the available anti-viral solution. Through collaboration with experimental researchers and further validation studies, we hope to translate these computational findings into tangible therapeutic interventions for COVID-19.

## Methodology

### Hardware and Software Used in this Study

The virtual screening was performed on the following computer system. 12<sup>th</sup> Generation Intel Core i5 Processor at 2.5 GHz 6 Cores 12 threads on Windows 11 Pro 64-bit operating system with 16 GB of RAM and a high-speed 1TB SSD was used for data storage. Furthermore, an Nvidia Dedicated GPU with 4 GB of memory utilized in this study to augment the hardware performance for parallel processing and expedited the conduction of the complex simulation. In this study, the virtual screening and analysis of the results furnished by the following software tools. PyRx 0.8 was used for the virtual screening process (<https://pyrx.sourceforge.io/>).<sup>61, 62</sup> PyRx is a user-friendly Virtual Screening software for Computational Drug Discovery, and It is conceived specifically for screening libraries of

compounds against potential drug targets. PyRx is targeted at Medicinal Chemists to seamlessly run Virtual Screening on their platforms with support from start to finish, from data preparation, molecular docking, and post-docking analysis. Although drug discovery is considerably more complicated, PyRx has a simple-to-use docking wizard, which essentially makes it a user-friendly computer-aided drug design software tool. Other helpful features of the PyRx software include a chemical spreadsheet-like interface and a robust visualization engine, which aided significantly in structure-based computer-aided drug design. Secondly, the Open Babel software was used for the conversion of chemical file formats and preprocessing of data. From the varied molecular file types, Open Babel piloted and unified the data for further analysis to the other software tool used in our study. Biovia Discovery Studio Visualizer was used to analyze the results. Biovia Discovery Studio Visualizer is a widely used tool for visualizing and analyzing molecular structures and protein-ligand interaction data (<https://discover.3ds.com/discovery-studio-visualizer-download>). The Biovia Discovery Studio Visualizer gave us the whole picture of the binding modes and molecular interactions of these target compounds to understand more about the mechanism of how our fruit compounds interact with Covid-19 target proteins.

#### **Sources of SARS-Cov-2 Proteins Structure**

The SARS-CoV-2 target proteins (Spike, MPro, RdRp, PLpro) were selected due to their key roles in viral entry, replication, and immune evasion. Inhibiting these proteins can effectively disrupt the virus's life cycle, making them ideal targets for lead molecule discovery. 3D structure of the most critical SARS-CoV-2 proteins were obtained from the Protein Data Bank (PDB) at <https://www.rcsb.org/>. It is a great source of molecular structure, and it is very beneficial for drug discovery research. The search was conducted in the search box using the PDB IDs of the specific protein structures. Moreover, four crucial proteins were selected for the research comprised of the Spike protein S protein with PDB ID 6M0J, Main protease MPro with PDB ID 7MB3, RNA- dependent RNA polymerase with the PDB ID 7B3D, and finally, Papain-like protease PLpro with the PDB ID 6WX4. After that, the 3D structure of these proteins were downloaded in PDB format, in order to ensure their accurate representation for the subsequent molecular docking and virtual screening

analyses. Finally, the downloaded PDB files are stored in the specific folder in proper organization, and they can be used for our required purposes.

#### **Sources of Small Molecules Structure (Fruit Compounds) and Reference Drug Molecules**

The 50 fruit-derived compounds were selected from kiwi, Grape, Pomegranate, and Black chokeberry based on known antiviral activity, presence of bioactive metabolites (flavonoids, polyphenols, tannins), and drug-likeness properties (Lipinski's Rule of Five, ADMET parameters). These fruits were chosen for their high antiviral potential and availability. PubChem (<https://pubchem.ncbi.nlm.nih.gov/>) was used as the principal source to acquire the small molecule structures obtained from fruit compounds, and reference drug molecules structures. A search process was performed to achieve the small molecule structure, which triggered the entry of small molecule names into the search box displayed on PubChem's initial webpage. A CID for each structure was used for the identification of the important information regarding each molecule. The structures of fifty small molecules from kiwi, Grape, Pomegranate, and Black chokeberry, as highlighted in Table S1, were acquired in the SDF format using the 3D conformer option. The process to download each small molecule structure was automatic thus; each acquired file was named as follows "Conformer3D\_COMPOUND\_CID\_XXX.sdf" where 'XXX' is the corresponding PubChem CID. After acquiring the SDF files, all downloaded molecules were organized carefully and stored in a folder referred to as "ligands". The approach was important because it enabled the acquisition of the small molecule structures passively from a readily available fruit, and their slicing purpose in our investigation of the lead molecule discovery for Covid-19 inhibitors through the virtual screening and molecular docking method.

#### **Protein Active Site (Binding Pocket) Identification**

Active site of the protein molecules were predicted in compliance to the protocol that was previously described using the web server [Version 3.0] (<http://sts.bioe.uic.edu/castp/index.html?2r7g>).<sup>63</sup> The protein molecules were first uploaded using the file option on the calculation panel, then the results were submitted. The results obtained were displayed in 3D with the active site residues of each binding site colored grey in the sequence section.

The active residues and all pockets were shown by clicking on both the pockets on the upper part of the page, and the box 'Show'. Clicking update was the next step, which was continued by making a click on the show pocket to reveal all the active pockets. The highest ranked was selected to find the optimal active site for the proteins, and this was then bundled and form the other positions.<sup>64</sup> The results within the data analysis protocol provided four forms of binding proteins which were further validated with the already reported data. In this study, Chain A was the binding pockets of Spike (S) protein (PDB ID: 6MOJ), Main protease (MPro) (PDB ID: 7AMJ), RNA-dependent RNA polymerase (PDB ID: 7B3D) respectively and Chain D was the binding pocket of Papain-like protease (PLpro) (PDB ID: 6WX4).

### Refinement of the Protein Structure

The refinement of protein structures plays a critical role in preparing these structures for conducting further molecular docking studies. The process implies a number of refinements and corrections performed to the initially obtained protein structures from the PDB. Specifically, the refinement and correction of protein structures were performed using BIOVIA Discovery Studio Visualizer software. The refined and corrected protein structures of all four protein molecules considered in our study emerge based on the following operations. First, the protein structures are opened using the 'Open' option available in the File Menu on the software. Next, to facilitate the consideration of the protein structure, the 'View' Menu is used, and the 'Hierarchy' option is selected. This helps to visualize the hierarchical arrangement of all components of the protein structure, allowing us to consider their details. Next, the extraneous water molecules are deleted from the protein structures using the 'Delete' option available in the Edit Menu. This operation is important because these water molecules do not interact directly with any possible inhibitor, and the provision of these water molecules into docking studies might distort the results of these simulations, introducing 'noise' into the software solutions. Similarly, all other heteroatoms composed of different non-protein atoms or molecules are deleted as well, employing the 'Delete' option available in the Edit Menu. This guarantees that only the protein structure is considered, and this protein structure is solely subjected to the molecular docking further in the study. Additionally, if there are some protein

chains that are also insignificant for our study and considered to be extraneous, these chains are also deleted using the 'Delete' option in the Edit Menu. This helps to consider only those parts of the protein that we believe are more crucial for the interaction with potential inhibitors in further studies. Additionally, for the purpose of preparing our protein structures for molecular docking, we also add the polar hydrogen atoms employing the 'add polar' option in the 'Hydrogen' submenu, available in the Chemistry Menu. The addition of polar hydrogen atoms is essential for further preparing the 3D structures of protein for considering the mechanisms of potential inhibitors' bonding to our protein target. Finally, the refined and corrected protein structures are saved as pdb-files using the 'Save As' option in the File Menu, which is also used in this course. Thus, the refinement of the protein structure guarantees that all extraneous elements are deleted, and the relevant hydrogen atoms are added to the protein, allowing us to prepare the refined and corrected protein structures to study the essential parts of fruit compounds obtained from common fruits and consider the mechanisms of their bonding with Covid-19 viruses.

### Preparation of Protein Structures for Molecular Docking

After the refined process, the proteins are converted from their initial PDB format to the PDBQT format, which is mandatory for the next docking study. This transformation was achieved through the following stepwise process. All the proteins were first loaded, through the 'Load Molecule' function, into the PyRx. The molecules were directly viewed on opening the PyRx home page, on the 'view panel', and each was labelled by the designated PDB ID (XXXX) where XXXX is unique four-character identifier for the proteins. These proteins were also reflected in the 'molecule' tab within the 'navigation panel'. The transformation of these proteins in facilitating docking was done through a set of actions. The process began with an action, a right-click, by any selected protein in the 'molecule', and was continued by selecting a range of options. Several steps emerged, after selecting 'AutoDock', which included clicking the 'Make macromolecule' operation. The action effectively transformed these proteins from their original 'PDB' format to the required 'PDBQT' format, which was ideal for the next docking step. The transformed

proteins were now in the PDBQT format and were all listed in 'AutoDock', in the navigation subpanel. Remarkably, this action was uniformly extended to all the proteins within the 'molecule' panel in a single row, and the same was repeated for all the proteins. This ensured that all the proteins were now converted and were listed in the 'AutoDock' subpanel, by unique PDB ID, with the appended '.pdbqt' format to the identified XXXX, and were listed as XXXX.pdbqt files.

### Preparation of Small Molecules for Virtual Screening

For the virtual screening of small molecules after downloading them, the process for their preparation was started by using "open babel." Several steps were performed carefully to make sure that the small molecules were successfully transformed. Initially, through the "open babel" tab, all the small molecules were selected and then "insert new item" was chosen for each molecule to load all of them in a stepwise manner. Moreover, through the "view" under "open babel" section, the loaded small molecules were seen, meeting their identities with their respective PubChem ID and molecular weight. In addition, it was made sure that the energy of each small molecule was minimized by selecting the PubChem ID and then right-click and "minimize all." Afterward, it was apparent that all the small molecules became energy minimized with the new nomenclature of 'pubchem id\_uff\_E.' In the subsequent step, to ensure that the preparation process was completed, the small molecules were converted to 'pdbqt' format. For the conversion, any of the energy-minimized small molecules was selected, and then right-click and "convert all to autodock ligand (pdbqt)," through which all the small molecules were converted to 'pdbqt' format. As a result, with the modified form of the small molecules, all these molecules were found in the "ligands" section of the "autodock wizard" of the "navigator" panel. Lastly, the names of the small molecules were shown with the extension of '.pdbqt' which made sure that the small molecules' preparation process had been successfully completed.

### Grid Box Generation for Docking

The dimensions of the receptor grid box were setup by using 'Autodock' embedded in PyRx.

As indicated in the 'Controls' panel at the bottom, 'Select molecule' tab and in 'Autodock' tab, we observed that "1 ligand selected" and the path of the chosen protein was displayed, respectively. To prepare the docking for all ligands, the 'Forward' button at the bottom right corner was clicked, and a grid box appeared on the display screen. By clicking the 'Molecules' tab on the right side, the "+" icon of the loaded protein was selected, allowing all residues in the chain to be visualized. The residues that bind were selected by right-clicking on the residue and going through the Display → Label → Atoms, and the atoms were shown in the protein. Finally, the grid box was adjusted to the desired dimensions that enclosed all selected residues, and the ligand was not required to be inside a grid box (see table 3 for the dimensions of the grid box and the active site residues).

### Virtual Screening and Molecular Docking using AutoDock Vina in PyRx 0.8

Structure-based virtual screening through molecular docking was performed using the 'AutoDock Vina',<sup>65,66</sup> which was incorporated in PyRx 0.8 (Welcome to the PyRx Website (sourceforge.io)). Initially, the process was started by using the 'Vina' wizard, and 'start' option was clicked. Consequently, the 'add ligand' and 'add macromolecule' options popped up, which enabled the selection of protein molecules. In order to perform the selection, the 'ctrl' bottom was hold while selecting all the small molecules presented in the 'AutoDock' wizard that was in the 'navigator' panel. The procedure continued by choosing and ensuring the selection of the identified protein molecules and small molecules, before starting the 'forward' option. The resultant 'view' provided the presentation of macromolecule and grid box, the latter being adjusted to ensure that all the active site binding residues is contained. The docking process was therefore initiated by clicking the 'forward' button the process implies that all the small molecules are being docked with the chosen protein molecules one after the other. The exhaustiveness value in Vina was set to 8 as it is the default value. The progression of the docking was monitored on the 'run Vina' wizard, as it displays the status when the docking is being performed and when it stayed 'completed' after the ligand is docked. Resultantly, the data was saved in .csv in Excel, through the 'save as comma-separated value' option in the

'Results' wizard. The same process is repeated for all the docking of small molecule library with all the proteins. Correspondingly, the docking of reference molecules was executed as described above with all the proteins. Consequently, the next phase was the evaluation of the results.

#### **Analysis of Docking Results in AutoDock [embedded in PyRx] and BIOVIA Discovery Studio Visualizer**

The analysis of docking results was performed based on AutoDock<sup>67</sup> and BIOVIA Discovery Studio Visualizer for each protein molecule and small molecules library. The findings led to the identification of the compound with the highest docking score, indicating the lowest binding energy, based on the data available in the Excel file created in the previous step. Further investigation of the findings included the use of both AutoDock through PyRx and BIOVIA Discovery Studio Visualizer. In the case of AutoDock, the 'macromolecules' option was identified in the navigator panel, and the 'out.pdbqt' was chosen as the output docked molecules. The next step included the right-click on one of the docked molecules, which resulted in the appearance of the 'display' option and the opening of all docked conformations of small molecules-protein. For the purposes of better visualization and analysis, the 'display' menu's 'molecular surface' option was chosen. Afterward, the optimal conformations were selected, and the structures were saved in .pdb format. Afterward, the saved conformations were analyzed using BIOVIA Discovery Studio Visualizer. In this case, the opening of the protein molecules from the docked complexes took place in 'Discovery Studio Visualizer,' followed by the activation of the 'hierarchy' in the 'view' menu. The previously saved docked complexes in the .pdb format were uploaded using the 'open' button identified in the file menu, and the 'view' menu's 'hierarchy' option was chosen. Afterward, mechanisms of the 'copy' and 'paste' were performed, leading to the replacement of the word 'hierarchy' with the docked complexes in protein structures. The final step involved the visualization of small molecules form within the protein binding pockets in their best-fit conformation. Next, the ligand was identified using the 'receptor-ligand interactions' menu's 'define receptor and ligand'

option. The detailed analysis of the ligand-protein interactions was performed using the 'display receptor-ligand interactions' option. The use of the 'ligand interactions' option helped identify various 2D and 3D diagrams illustrating the details of ligand-protein interactions and presenting different types of interactions to facilitate the interpretation. Other findings were analyzed through the 'display receptor surface' option.

#### **ADMET (Absorption, Distribution, Metabolism, Excretion, and Toxicity) Analysis using ADMET Lab 3.0**

One of the most vital tasks conducted as a part of this research is the profound assessment of Absorption, Distribution, Metabolism, Excretion, and Toxicity properties of the chosen small molecules. An ADMET analysis is critical in the course of drug design as it helps select those options with the best pharmacokinetic and pharmacodynamic profiles, thus making the drug developing process more likely to succeed. In this research, such an analysis was created with the help of ADMETLab 3.0, using a standard procedure described elsewhere.<sup>68-70</sup> The first step in this ADMET analysis process was to access ADMETLab 3.0 by following the given link (<https://admetlab3.scbdd.com/>) and, on the homepage, accessing the 'services' menu and choosing 'ADMET Screening.' The next step was to obtain the Simplified Molecular Input Line Entry System (SMILES) string of the molecule of choice [Top ten high scoring molecules]. For that, PubChem database was used. Finally, the SMILES obtained were used to 'SMILES' option in the functionality of ADMET Screening to begin the analysis. The process itself was initiated by clicking 'Run' that launches ADMETLab 3.0 to assess Absorption, Distribution, Metabolism, Excretion, and Toxicity options for each and every molecule used. After the analysis was completed, the table was shown with the results and the information about the molecule underneath it. For the profound examination of the process, the 'view' for each option was used. Finally, results were downloaded in 'csv' format to be further studied with the help of Excel. Such a meticulous process was pivotal in not only learning about the potential pharmaceutical utility of the given compounds but also in preparing to the next stages of drug development process.





checkpoint actions in COVID-19 combating. This factor is because: Also MPro's potential spectrum of activity could be a potent target for drug design due to the higher transcriptase complexity for these viral proteins. Second, inhibiting MPro could also halt the entire viral replication and alleviate panorganism transmission. Lastly, MPro has a less likelihood of functional mutation compared with different viral proteins, thus a lower risk of drug-resistant developing.<sup>73</sup> Therefore, the drug discovery process for the docking of small molecule libraries with the protease designed for the inhibition of Main Protease's activity in SARS-CoV-2 could lead to efficient candidates for the broad-spectrum control of infection without the universal tendency to functional mutation by the SARS-CoV-2 virus. Our docking analysis, fifteen molecules have shown higher affinity from the interaction with the MPro. This is demonstrated by their low negative docking energy scores relative to the reference approved drugs.

scored the highest negative energy of -9.2 kcal/mol exploited six conventional hydrogen bonds with residues Asn142 (2), Glu166 (2), and Thr26 (2). It also formed two carbon hydrogen bonds with Cys145 and Gln189 and a pi-sulphur bond with Cys145 and two pi-pi stacking interactions with His41, and two pi-alkyl bonds with Met165. Second, the compound 12137509 also established hydrogen bonds with Phe140 and Glu166, a carbon-hydrogen bond with Met165, a pi-sulphur bond with Cys145, two pi-pi stacking interactions with His41, and two pi-alkyl bonds with Cys145 and Met165. Finally, the compound 5280805 formed five conventional hydrogen bonds with residues Gln110 (1), Thr111 (1), Asn151 (1), Arg105 (1), and Pro108 (1), and a pi-alkyl bond with Val104. Furthermore, all these fifteen compounds indicated higher binding energy interactions and negative bonding energy scores compared to the reference drugs. These outcomes might promote future research in the design of novel coronavirus inhibitors and their derivatives.

As shown in Fig. 4, the top three molecules exploited significant interactions with the proteins: First, the compound (Pubchem Id 44256718)

#### Docking Result Analysis of Small Molecule Library with RdRp Protein

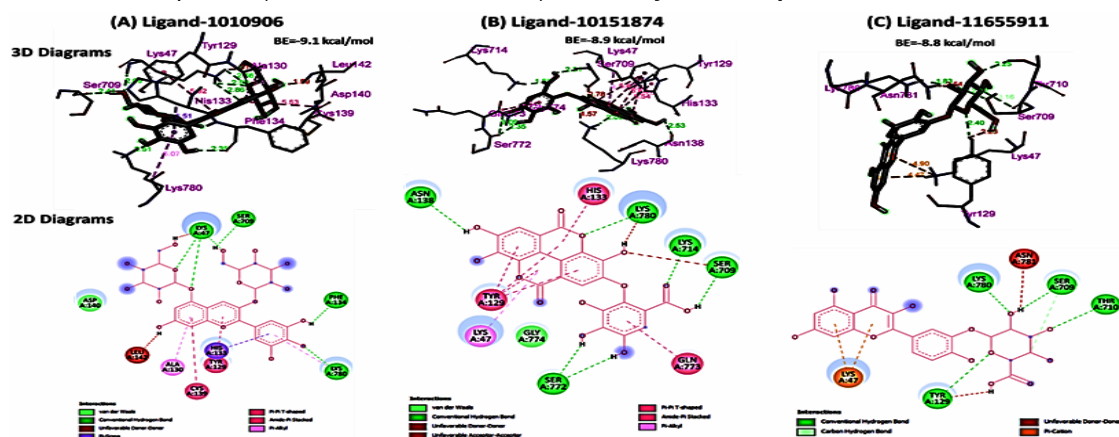


Fig. 5. 3D and 2D docking interactions of top three high scoring compounds with RdRp Protein (PDB ID: 7b3d) [BE=Binding Energy]

RNA dependent RNA polymerases (RdRp) are essential enzymes for the replication of Covid-19 and other RNA viruses, involved in the synthesis of RNA strands using the RNA templates. It is crucial for the replication and proliferation of the virus inside host cells, where the RdRp promotes the replication of the viral RNA genome leading to the infection. For remarkable drug design, RdRp is an ideal target for drug development, given its binding during the replication of the viral RNA which is vital for the survival of the virus. Inhibiting the activity of the RdRp

would disrupt the synthesis of the viral RNA thereby preventing the continued replication and spread of the virus. The result would be a reduction in infection, and hence RdRp proves to be a remarkable current target for developing antiviral drugs for Covid-19. The binding seems conservative among different RdRp viral strains, and its role in viral replication suggests it is an appealing target to approach the Covid-19 pandemic.<sup>74-76</sup> The matching of the small molecule library with RdRp in the docking results revealed some exciting findings, as presented.

Firstly, the compound having the PubChem ID 1010906 gave the highest docking score of -9.1 kcal/mol. This molecule established seven conventional hydrogen bonds with Lys47 (4 interactions), Lys780, Ser709, Phe134, as well as a pi-sigma interaction with His133, a pi-pi T-shaped interaction with Tyr129, and an amide-pi stacked interaction with Cys139 and Asp140. Moreover, two pi-alkyl interactions with Ala130 and Lys780 were recognized. Compound 10151874 also delivered a high docking score of -8.9 kcal/mol, engaged in six conventional hydrogen bonding interactions involving Lys714, Lys780, Ser709, Ser772 (2 interactions), Asn138, as well as five pi-pi T-shaped interactions with Tyr129, and His133, amide-pi stacked interaction with Gln773 and

Gly774, and pi-alkyl interaction with Lys47. Finally, Compound 11655911 demonstrated a docking score of -8.8 kcal/mol, established four conventional hydrogen bonds with Tyr129, Thr710, Lys780, and Ser709, one carbon-hydrogen interaction with Ser709, and two pi-cation interactions with Lys47. Notably, all these compounds demonstrate a high-level binding affinity and docking score against RdRp compared to the FDA approved reference drug molecules. Therefore, the combination along with their respective derivatives has the potential to facilitate the design of new Covid-19 inhibitors.

### Docking Result of Small Molecule Library with PLpro

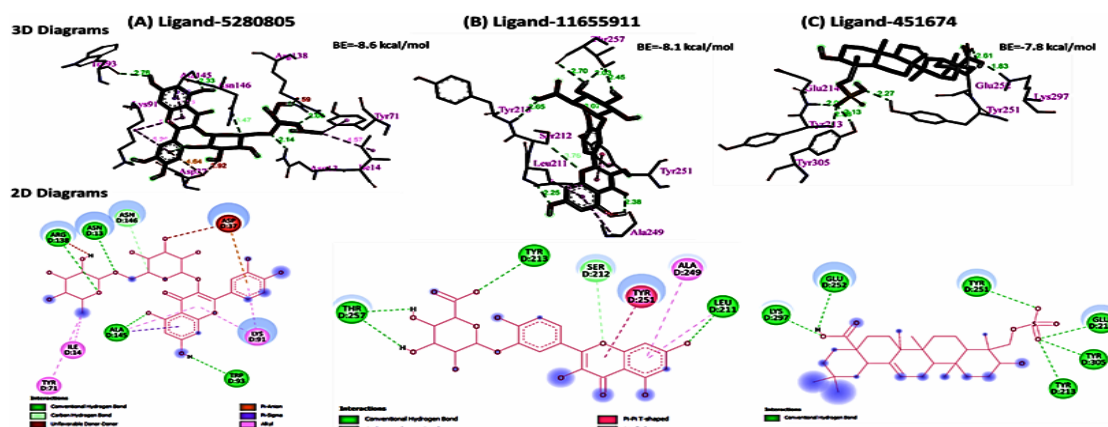


Fig. 6. 3D and 2D docking interactions of top three high scoring compounds with PLpro Protein (PDB ID: 6wx4) [BE=Binding Energy]

Covid-19 pathogenesis involves the action of Papain-like protease due to being one of the vital proteases of the SARS-CoV-2 encoding protein. This protease is responsible for the processing of the viral polyproteins necessary for replication and maturation of the virus. The importance of its binding is attributed to the ability to cleave the viral polyprotein in specific areas of the amino acid row, leading to the release of functionally active viral proteins necessary for the viral assembly and infection. Targeting of PLpro for drug design is a much-promising strategy for novel drugs against the virus's cycle, where the inhibition of the protease leads to the impossibility of cleavage of polyprotein and the reduced infectivity of the virus. The progression of the Covid-19 viral factor can be reduced due to the decreased viral load. As PLpro is a virus's structural unit, drugs targeting this enzyme are likely to contribute to fewer side effects on the host cell.<sup>77-79</sup> Sixteen small molecules showed evident better binding properties with PLpro, verified

by negative docking scores compared to reference drug molecules.

Small molecule 5280805 from PubChem has the best identified docking score of -8.6 kcal/mol. This molecule forms four conventional hydrogen bonds with the protein amino acid, namely Asn13, Arg138, Ala135, and Trp93, a carbon-hydrogen (CH) bond with Asn146, and pi-anion and pi-sigma interaction with Asp37 and Ala145, respectively. Moreover, hydrophobic and pi-alkyl interaction is maintained through Ile14, Tyr71, Lys91 (two interactions), and Ala145, respectively. Similarly, compound ID 11655911 with a docking score of -8.1 kcal/mol forms seven conventional hydrogen bonds with Leu211, Tyr213 (two interactions), and Thr257, a CH bond with Ser212, and pi-pi T-shaped interactions with Tyr251 as well as pi-alkyl interactions with Leu211 and Ala249. Compound ID 451674 with a docking score of -7.8 kcal/mol

forms six conventional hydrogen bonds with Tyr213, Glu214, Tyr251, Lys297, Tyr305, and Glu252. These compounds exhibit superior binding affinity and docking scores compared to FDA-approved reference drugs, suggesting their potential in facilitating the design of novel Covid-19 inhibitors and their derivatives.

### Interpretation of Docking Results Comparing with FDA Approved Drug Molecules

The analysis of docking results for the FDA-approved drug molecules with the protein targets show interestingly interacting proteins.<sup>80-82</sup> As shown in Fig. 7 shows the 3D and 2D images of interaction between drug molecule is shown with highest score with the proteins. Among the 4 FDA-approved drugs *Nirmatrelvir* (Pubchem id: 155903259) exhibits highest binding affinity with spike proteins shows highest docking score of -8.1 kcal/mol. In this interaction it involves 2 Conventional hydrogen bond interactions with Tyr385 and Phe 390, also 3 carbon-hydrogen bond interaction with Arg393, Ala348 and Arg393 and pi-sigma with His401 and Trp349, 2 pi-alkyl with Trp349 and His401. The reference drug molecule Remdesivir (Pubchem id: 121304016) also

shows support with the Main protease with highest docking score of -8.0 kcal/mol. This molecule exhibits 4 Conventional hydrogen bonding interactions with Phe294, Thr111, Ser158 and two carbon-hydrogen bond interaction with Thr292 and Pro293, also amide Pi-stacked with Phe294 and Pro293, and hydrophobic alkyl interaction with Val202. As well as, in case of PLpro receptor *Nirmatrelvir* also exhibit the highest score with the docking value 7.7 kcal/mol. This molecule exhibits electrostatic attractive charge interaction with Glu318, Conventional hydrogen bond with Leu317, a hydrophobic alkyl interaction with Val188, pi-alkyl interaction with Tyr233. For RdRp receptor *Nirmatrelvir* exhibits the same score of -7.7 kcal/mol and shows one hydrogen bond with Lys47, four carbon-hydrogen bonds with Tyr129, Thr710, Asp711 and Ala130, oxygen-halogen interaction with His133 and Hydrophobic Pi-sigma with Tyr32. With comparison to the small molecule library containing several numbers of fruit compound shows high binding affinities and docking score when compares with the FDA-approved reference drug molecules Table 1. Hence, it can easily understand the potential biological activity of fruit compounds and their derivatives to design a novel Covid-19 inhibitors.

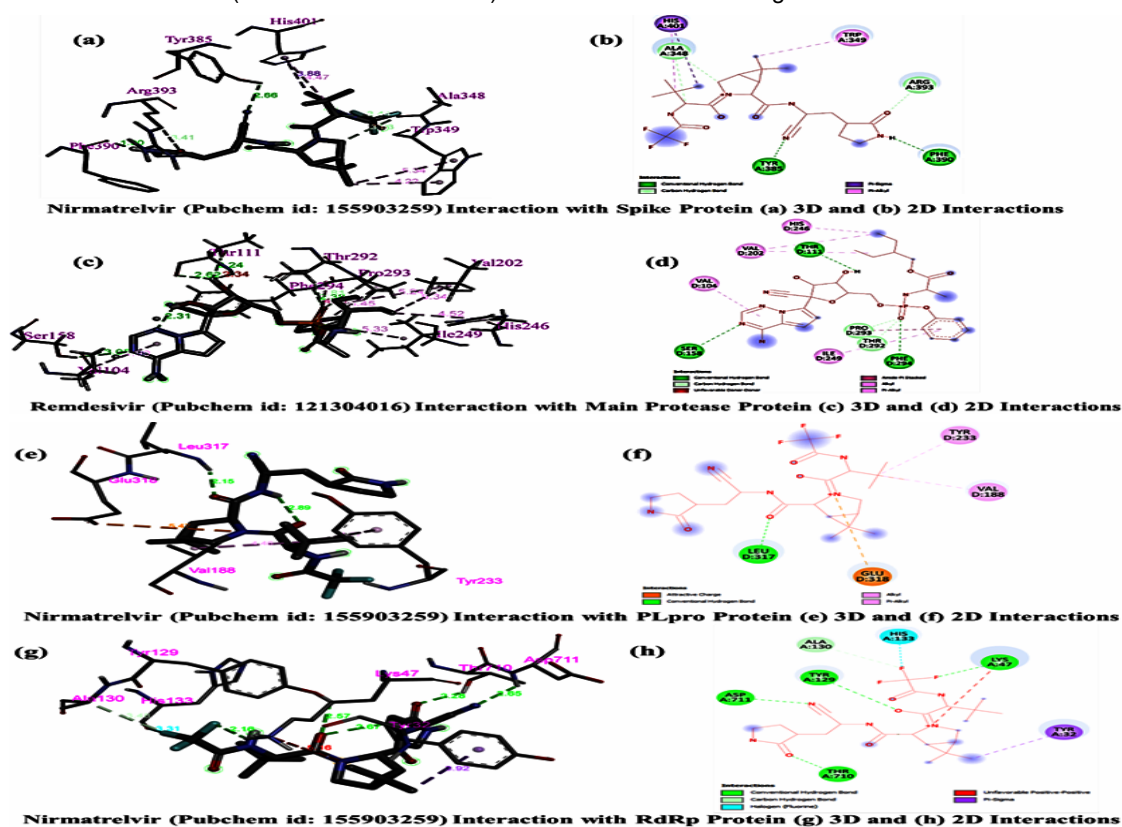


Fig. 7. 3D and 2D docking interactions of top scoring FDA Approved drugs (reference compounds) with four SARS-Cov-2 proteins

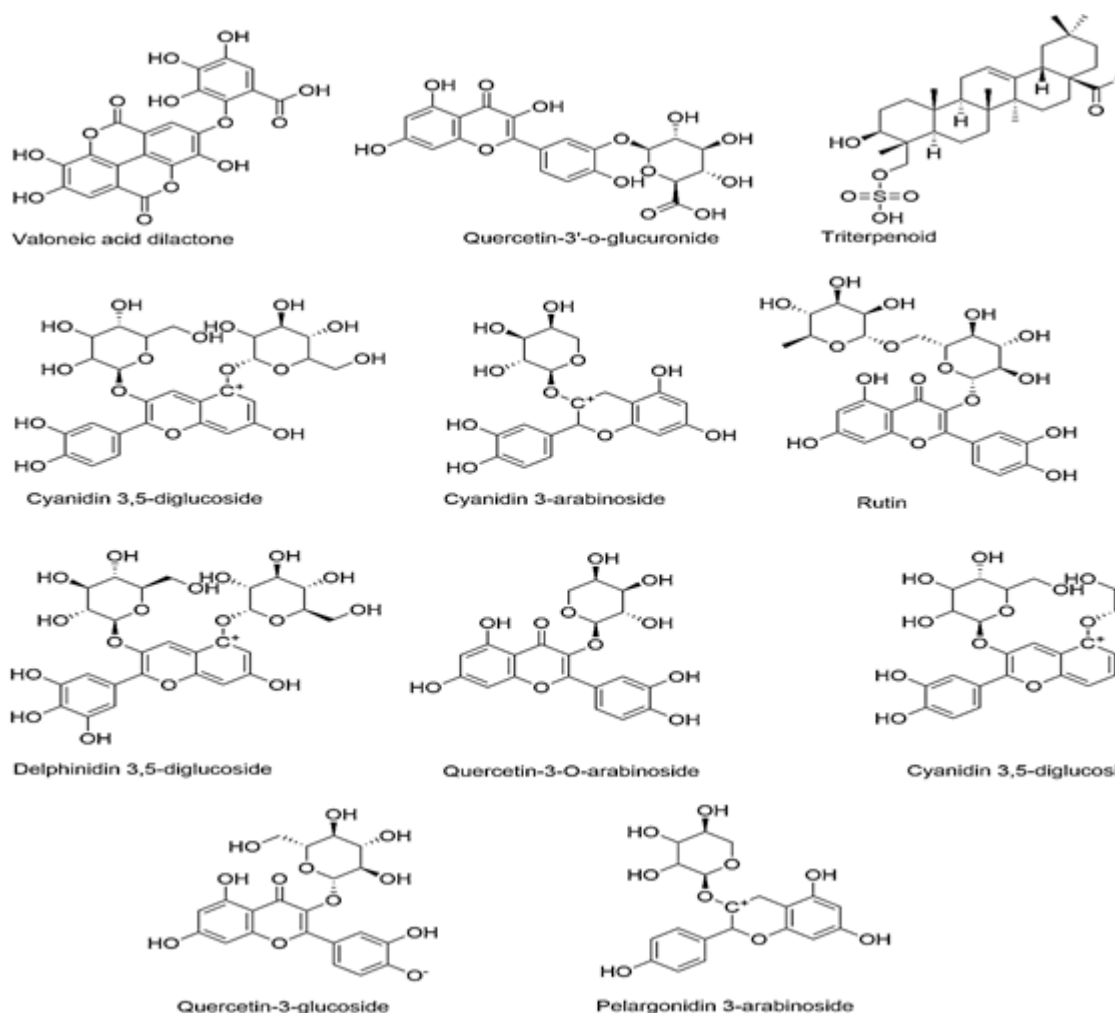


Fig. 8. Chemical Structure of the selected high scoring ligands [see supporting information for structure of all the molecules and their sources]

### Overall mechanistic insights

Overall, the virtual screening and molecular docking analysis of fifty small molecules against four key SARS-CoV-2 proteins provided important discoveries in terms of possible mechanisms of their actions and avenues for medical intervention. Some small molecules exhibited outstanding binding affinity with extremely low docking scores compared to the reference drugs already approved by FDA for the same targets. For example, PubChem ID 10151874, 44256718, and 11655911 provided excellent results for all the proteins involved and scored between -9.0 and -9.7 kcal/mol. These related small molecules interacted with multiple bonds including conventional hydrogen bonds with the key residues to pi-alkyl, pi-cation, and pi-pi stacking interactions. Further, 10151874 formed seven hydrogen bonds within the

S protein that indicates the very strong molecular interactions likely contributed to the high score. The compound 44256718 showed six hydrogen bonds with MPro and seven with RdRp which indicates its diverse potential for interactions with targets. The observed activity level was above the reference drugs, which makes the provided small molecules good candidates for the COVID-19 inhibitors.

From a structural perspective, these small molecules have a wide range of interaction profiles with the target proteins, all of which may have contributed to the binding affinities. In particular, small molecules with high docking scores were able to form more hydrogen bonds to one or more critical residues, increasing the overall stability within the binding pocket. Hydrophobic interactions such as

pi-alkyl and pi-pi stacking add to this binding affinity by allowing the small molecules to have a favorable interaction to the hydrophobic residues on the protein. The observation of pi-sigma, pi-cation interactions as well as other types of interactions makes it clear that these small molecules have structural variability that allows them to have interactions with different amino acid residues of the target protein. In conclusion, the structural perspective offered many ways of understanding the mechanism of action of these drugs and how they can further be optimized.

The results of the interaction of the fifty small molecules with the key SARS-CoV-2 proteins through the virtual screening and molecular docking analysis have provided insightful mechanistic information into the potential COVID-19 inhibitors.

In several cases, the binding affinity of PubChem ID 10151874, 44256718, and 11655911 molecules for multiple protein targets was remarkably high compared to FDA-approved reference drugs. The molecules engage in various interactions with the target proteins, such as hydrogen bonds, pi-alkyl, and pi-pi stacking, which is likely to explain their high binding affinity and potential therapeutic activity. The small molecules engaged with diverse interaction profiles due to their structural differences, indicating that different amino acid residues can be targeted. In conclusion, the high binding affinity of the identified small molecules suggests their potential as lead compounds for the development of new COVID-19 inhibitors, requiring further experimental verification and optimization for clinical administration.

**Table 1: Comparison of Binding Energy of Top Ten High Scoring Small Molecules and Reference Drug Molecules with SARS-COV-2 Proteins**

Spike Protein (6m0j)			PLpro (6wx4)		
PubChem ID	Small molecule	Binding affinity (kcal/mol)	PubChem ID	Small Molecule	Binding Affinity (kcal/mol)
10151874	Valoneic acid dilactone	-9.7	35280805	Rutin	-8.6
11655911	Quercetin-3'-o-glucuronide	-9.1	11655911	Quercetin-3'-o-glucuronide	-8.1
451674	Triterpenoid	-9	451674	Triterpenoid	-7.8
5281855	Ellagic acid	-8.7	10151874	Valoneic acid dilactone	-7.7
5280805	Rutin	-8.7	35281718	t-Piceid	-7.5
44256718	Cyanidin 3,5-diglucoside	-8.6	12309865	Quercetin-3-O-arabinoside	-7.4
10100906	Delphinidin 3,5-diglucoside	-8.6	1794427	Chlorogenic Acid	-7.4
5281792	Rosmarinic acid	-8.5	441699	Cyanidin 3-galactoside	-7.3
5281718	t-Piceid	-8.5	3280445	Luteolin	-7.3
5281672	Myricetin	-8.5	3281792	Rosmarinic acid	-7.3
Reference FDA Approved Drugs [highest docking score]			Reference FDA Approved Drugs [highest docking score]		
155903259	<i>Nirmatrelvir</i>	-8.1	121304016	Remdesivir	-8
Main Protease (7mb3)			RdRp (7b3d)		
PubChem ID	Small Molecule	Binding Affinity (kcal/mol)	PubChem ID	Small Molecule	Binding Affinity (kcal/mol)
44256718	Cyanidin 3,5-diglucoside	-9.2	1010906	Delphinidin 3,5-diglucoside	-9.1
12137509	Cyanidin 3-arabinoside	-8.9	10151874	Valoneic acid dilactone	-8.9
5280805	Rutin	-8.9	11655911	Quercetin-3'-o-glucuronide	-8.8
4481259	Cyanidin 3-galactoside	-8.8	44256718	Cyanidin 3,5-diglucoside	-8.7
25203368	Quercetin-3'-galactoside	-8.8	5281718	t-Piceid	-8.6
12309865	Quercetin-3-O-arabinoside	-8.8	4481259	Cyanidin 3-glucoside	-8.5
11655911	Quercetin-3'-o-glucuronide	-8.7	5281855	Ellagic acid	-8.4
10100906	Delphinidin 3,5-diglucoside	-8.6	441699	Cyanidin 3-galactoside	-8.3
44256694	Pelargonidin 3-arabinoside	-8.6	5320457	Pelargonidin 3-O-glucoside	-8.3
10151874	Valoneic acid dilactone	-8.5	451674	Triterpenoid	-8.1
Reference FDA Approved Drugs [highest docking score]			Reference FDA Approved Drugs [highest docking score]		
155903259	<i>Nirmatrelvir</i>	-7.7	155903259	<i>Nirmatrelvir</i>	-7.7

Some compounds exhibited superior binding affinities across multiple SARS-CoV-2 protein targets due to their structural flexibility, diverse functional groups, and strong molecular interactions. The ability

of these compounds to bind effectively to different proteins is largely influenced by the presence of multiple hydrogen bond donors and acceptors, aromatic rings, hydrophobic regions, and charged

functional groups, which facilitate interactions with critical amino acid residues in the active sites of these proteins. For example, PubChem ID 10151874 (-9.7 kcal/mol) demonstrated excellent binding with the Spike (S) protein due to its multiple hydrogen bonding interactions with residues like Gln98, Lys562, and Tyr202, along with additional pi-alkyl interactions that enhanced stability within the binding pocket. Similarly, PubChem ID 44256718 (-9.2 kcal/mol) exhibited strong binding with both Main Protease (MPro) and RNA-dependent RNA Polymerase (RdRp), forming a combination of hydrogen bonds, pi-pi stacking, and hydrophobic interactions, which contributed to its high affinity across different targets.

The ability of these compounds to adapt to different binding sites is a key factor in their performance. Some small molecules possess a rigid yet adaptable scaffold, allowing them to align favorably with various active sites despite differences in protein structure. Additionally, the presence of electron-rich functional groups, such as hydroxyl, carbonyl, and aromatic systems, enables stronger electrostatic interactions and pi-stacking with residues within the binding pocket. These interactions contribute to a lower free energy of binding, making these compounds highly effective inhibitors. The superior performance of certain fruit-derived compounds across multiple SARS-CoV-2 targets can be attributed to their structural diversity, ability to form multiple stabilizing interactions, and adaptability to different protein conformations. These findings underscore the potential of such molecules as broad-spectrum inhibitors, offering promising leads for antiviral drug development.

The superior binding affinities of the top-performing fruit-derived compounds can be attributed to a combination of hydrogen bonding, pi-pi stacking, and hydrophobic interactions, which collectively enhance stability within the active sites of SARS-CoV-2 proteins. Hydrogen bonds play a crucial role in ligand-protein interactions by stabilizing the complex, as seen with PubChem ID 10151874, which formed seven hydrogen bonds with Spike protein residues (Gln98, Lys562, Tyr202), significantly enhancing its binding affinity (-9.7 kcal/mol). Similarly, PubChem ID 44256718 demonstrated strong interactions with MPro (-9.2 kcal/mol) through hydrogen bonds with catalytic residues such as Asn142 and Glu166, making it an effective inhibitor. Pi-pi stacking and pi-cation interactions further contributed to stability, with molecules like PubChem ID 11655911 forming

pi-stacking interactions with His378 in Spike protein and His41 in MPro, reinforcing ligand positioning within the active site. Additionally, hydrophobic interactions, such as those observed in PubChem ID 5280805 (interacting with Leu95, Val209, Ala396 in Spike protein), further anchored the ligands in their respective binding pockets, enhancing stability. These multi-faceted interactions explain why these compounds outperformed FDA-approved inhibitors like *Nirmatrelvir* (-8.1 kcal/mol), demonstrating their strong potential as lead molecules for COVID-19 therapy.

#### **Potential Resistance Mechanisms and Adaptability to Viral Mutations**

Given the high mutation rate of SARS-CoV-2, resistance to antiviral inhibitors remains a major concern, particularly for synthetic drugs that often target a single conserved residue, making them vulnerable to mutations. However, fruit-derived compounds demonstrated resilience against potential resistance mechanisms by binding to multiple residues across different viral proteins, reducing the likelihood of complete loss of activity. For example, PubChem ID 10151874 and 44256718 exhibited binding across multiple viral proteins, ensuring robust inhibition even if mutations alter a few key residues. Unlike conventional inhibitors that may lose efficacy due to point mutations in druggable pockets (e.g., MPro and RdRp mutations), the compounds in this study engaged with highly conserved regions, enhancing their adaptability. Additionally, the structural flexibility of polyphenol-rich molecules, such as those from Grapes and Pomegranates, enables them to accommodate conformational changes in viral proteins. However, to further assess resistance potential, molecular dynamics simulations are recommended to evaluate the stability of these ligand-protein interactions under different conditions. Future *in vitro* and *in vivo* studies, including enzyme inhibition assays, cytotoxicity testing in human lung epithelial cells, and animal model validation, will be essential to confirm the effectiveness of these compounds against evolving SARS-CoV-2 variants.

#### **ADMET Analysis**

ADMET analysis is an imperative component in drug likeness studies which helps avoid those entities that are likely to fail in a real setting due to unwanted pharmacokinetic and pharmacodynamic consequences. A set of rules and parameters guide predictions upon how likely a certain compound is going to make a drug. For

example, Pfizer rules, more commonly referred to as the 'Rule of Five', demonstrated that any molecule intended to act as a drug should not weigh more than 500mw, not have more than 5 hydrogen bond donors, not more than 10 hydrogen bond acceptors and its logP value should not be above 5. Similarly, golden triangle rules dictate that a great drug must balance between lipophilicity, size and polarity. Lipinski's rule, a very common guideline, explains that oral bioavailability drugs tend not to violate more than one of the following four parameters: molecular weight, hydrogen bond donors, hydrogen bond acceptors and lipophilicity. Pain alerts on the other hand will keep a chemist from assessing a serving outcome compound but carry a risk of elevated counts of wrong positives within the vast screening outcomes. GSK rules, focus on recognizing possible liabilities, whether potential metabolic spices or reactive groups, that should be avoided whatsoever. Additionally, logP and logD will give the lipophilicity and distribution properties helping to alter ameability, distribution, metabolism and excretion style. Synthetic accessibility score measures the stuff the facile to make shocked by the ease this style the compound can be reloaded. How well a drug can enter the brain from the body has to be kept in mind and added at the site.<sup>83,84</sup>

chosen and subjected to further pharmacokinetic analysis, including absorption, distribution, metabolism, excretion, and toxicity study. This study was carried out using the ADMETlab (version 3.0) druglikeness analysis tool. In the druglikeness study, all the molecules selected adhered to Pfizers' rule, all having more than 90% as per the golden triangle rules. Half of the molecules followed the Lipinski rule, 40% of the molecules had no PAINS alert, and the rest of the molecules had one PAINS alert. Toxicity study revealed the cytotoxic to non-cytotoxic effect for most molecules. Other molecules were found to adhere to the GSK rule, with more than half showing slight to non-binding to the macromolecules and better membrane permeability. This is reported by the logP value which falls within the range of <0 -3, a clear indication of enough binding affinity from their high negative docking scores. Additionally, LogD value was <1-3 for all the molecule, indicating good balance with their hydrophilicity or hydrophobicity, then the synthesis accessibility score for all the molecules was <5, showing the ease of synthesis. Some of the molecules have limited ability to traverse the blood-brain barrier (BBB) through the BBB value were <0.5. This is similar to excretion from the body, where clearance (CL) value>5 was exhibited by more than 90% of the molecules. Therefore, all the molecules exhibited good druglikeness, and there is an exception regarding the parameter measured.

Molecules with high docking scores were

**Table 2: Selected ADMET data of high scoring ligands**

Pubchem ID	Molecule Name	LogD	LogP	HIA	BBB	PPB	CL	PAINS	Lipinski	Pfizer	GSK	GoldenTriangle
10151874	Valoneic acid dilactone	0.481	1.301	0.794	0.007	85.26%	1.715	1	Rejected	Accepted	Rejected	Accepted
131750813	Quercetin-3-O-glucuronide	-0.163	-0.807	0.326	0.115	76.75%	1.19	0	Rejected	Accepted	Rejected	Accepted
451674	Triterpenoid	3.797	3.714	0.781	0.17	98.45%	1.114	0	Accepted	Accepted	Rejected	Rejected
5281855	Ellagic acid	0.794	1.117	0.198	0.011	78.23%	2.346	0	Accepted	Accepted	Accepted	Accepted
5280805	Rutin	0.695	-0.763	0.925	0.111	83.81%	1.349	1	Rejected	Accepted	Rejected	Rejected
44256718	Cyanidin-3,5-diglucoside	0.414	-1.2	0.986	0.465	76.81%	1.89	1	Rejected	Accepted	Rejected	Rejected
10100906	Delphinidin-3,5-diglucoside	0.154	-1.433	0.978	0.437	78.26%	1.685	1	Rejected	Accepted	Rejected	Rejected
5281792	Rosmarinic acid	1.65	1.775	0.231	0.049	97.72%	1.535	1	Accepted	Accepted	Accepted	Accepted
5281718	L. Flavolid	1.286	1.112	0.646	0.362	97.06%	2.545	0	Accepted	Accepted	Accepted	Accepted
5281672	Myricetin	0.9	1.747	0.893	0.060	92.77%	1.716	0	Accepted	Accepted	Accepted	Accepted
12137509	Cyanidin-3-arabinoside	1.725	0.913	0.729	0.041	91.46%	0.693	1	Accepted	Accepted	Rejected	Accepted
12303220	Cyanidin-3-glucoside	1.163	0.097	0.823	0.069	87.23%	9	0	Accepted	Accepted	Rejected	Accepted
25203368	Quercetin-3-glucoside	00.948	-0.17	0.766	0.048	88.41%	1.289	0	Rejected	Accepted	Accepted	Accepted
12309865	Quercetin-3-O-arabinoside	1.066	0.522	0.660	0.082	89.27%	2.929	0	Rejected	Accepted	Accepted	Accepted
44256694	Pelargonidin-3,5-diglucoside	2.195	1.564	0.793	0.057	85.92%	1.601	0	Accepted	Accepted	Accepted	Accepted
176457	Cyanidin-3-galactoside	1.163	0.097	0.823	0.069	87.23%	9	0	Accepted	Accepted	Rejected	Accepted
5320457	Pelargonidin-3-O-galactoside	1.066	0.578	0.783	0.062	86.03%	0.971	0	Accepted	Accepted	Accepted	Accepted

**Table 3: Grid box details and binding residue of SARS-Cov-2 Proteins**

Protein Name	Grid Box Size (Vina Search Space)	Binding Residue
Spike Protein (6m0j)	Center: X = -24.0470, Y = 19.5419, Z = -28.7720 Dimension (Angstrom): X = 65.3101, Y = 71.7714, Z = 70.0034	Gln98, Gln102, Lys562, Trp566, Tyr202, Asp206, Glu564, Leu95, Val209, Ala396, Tyr196, Ala99, Gly395, Asn397, His401, Arg393, Asp350, Arg514, His378, Ala348
Main Protease (7mb3)	Center: X = 18.7488, Y = 0.3664, Z = -50.8550 Dimension (Angstrom): X = 70.8220, Y = 55.6672, Z = 46.1485	Asn142, Glu166, Thr26, Cys145, Gln189, His41, Met165, Gln110, Thr111, Asn151, Arg105, Pro108, Val104.
RdRp (7b3d)	Center: X = 98.1129, Y = 102.6207, Z = 93.5719 Dimension (Angstrom): X = 81.9481, Y = 85.6788, Z = 79.8943	Lys47, Lys780, Ser709, Phe134, His133, Tyr129, Cys139, Asp140, Ala130, Lys714, Ser709, Ser772, Gln773, Gly774, Thr710.
PLpro (6wx4)	Center: X = 0.6512, Y = -18.4856, Z = -33.9966 Dimension (Angstrom): X = 57.0063, Y = 46.1581, Z = 93.0772	Asn13, Arg138, Ala135, Trp93, Asn146, Asp37, Ala145, Ile14, Tyr71, Lys91, Leu211, Tyr213, Thr257, Ser212, Tyr251, Leu211, Ala249, Tyr213, Glu214, Lys297, Tyr305, Glu252.

### CONCLUSION

This study identified small molecules with potential to inhibit SARS-CoV-2, showing superior docking scores and molecular interactions compared to FDA-approved antivirals. Notably, PubChem ID compounds 10151874, 44256718, and 11655911 exhibited strong binding affinities due to hydrogen bonding, pi-alkyl, and pi-pi stacking interactions. Molecular docking suggested their ability to target key viral replication sites, while ADMET analysis confirmed favorable pharmacokinetics, including low toxicity and good bioavailability. Further validation through *in vitro* assays, *in vivo* pharmacokinetic studies, and molecular dynamics simulations is necessary. Structural flexibility studies could assess their adaptability to viral mutations. These bio-derived compounds present cost-effective, less toxic

alternatives to synthetic inhibitors, highlighting the need for interdisciplinary research in drug design and molecular pharmacology. Future work will focus on structural optimization and *in vivo* screening to translate these computational findings into therapeutic applications..

### ACKNOWLEDGMENT

The authors thank Institute of Engineering & Management Kolkata, University of Engineering & Management Kolkata for providing Financial Support and all necessary facilities required for carrying out the research successfully. The Work was financially supported from the Grant-in-Aid research grant given by IEM Kolkata.

### Conflict of Interest

The authors declare no conflict of interest.

### REFERENCES

- Ciotti, M., The COVID-19 pandemic., *Critical Reviews in Clinical Laboratory Sciences*, **2020**, 57(6), 365-388. DOI: <https://doi.org/10.1080/10408363.2020.1783198>.
- El-Shabasy, R.M., Three waves changes, new variant strains, and vaccination effect against COVID-19 pandemic., *International Journal of Biological Macromolecules.*, **2022**, 204, 161-168. DOI: <https://doi.org/10.1016/j.ijbiomac.2022.01.118>.
- Kanduc, D. and Y. Shoenfeld, On the molecular determinants of the SARS-CoV-2 attack., *Clinical Immunology (Orlando, Fla.)*, **2020**, 215, 108426. DOI: <https://doi.org/10.1016/j.clim.2020.108426>.
- Abulsoud, A.I., Mutations in SARS-CoV-2: Insights on structure, variants, vaccines, and biomedical interventions., *Biomedicine & Pharmacotherapy.*, **2023**, 157, 113977. DOI: <https://doi.org/10.1016/j.biopha.2022.113977>.
- Pérez-Vargas, J., Discovery of lead natural products for developing pan-SARS-CoV-2 therapeutics., *Antiviral Research.*, **2023**, 209, 105484. DOI: <https://doi.org/10.1016/j.antiviral.2022.105484>.
- Jackson, C.B.; M. Farzan, B. Chen, and H. Choe, Mechanisms of SARS-CoV-2 entry into cells., *Nature Reviews Molecular Cell Biology.*, **2022**, 23(1), 3-20. DOI: <https://doi.org/10.1038/s41580-021-00418-x>.

7. Shang, J., Cell entry mechanisms of SARS-CoV-2., *Proceedings of the National Academy of Sciences.*, **2020**, 117(21), 11727-11734. DOI: <https://doi.org/10.1073/pnas.2003138117>.
8. Wang, S.; G. Dong, and C. Sheng, Structural simplification: an efficient strategy in lead optimization., *Acta Pharmaceutica Sinica B.*, **2019**, 9(5), 880-901. DOI: <https://doi.org/10.1016/j.apsb.2019.05.004>.
9. Barcelos, M.P., Lead optimization in drug discovery, in *Research Topics in Bioactivity, Environment and Energy: Experimental and Theoretical Tools*. **2022**, Springer. 481-500.
10. Shivani Sharma, A.C.; Mujahed N Pathan and Shivam Tyagi., AI-powered virtual screening for drug discovery: Methods and challenges., *Int. J. Pharm. Pharm. Sci.*, **2024**, 6(2), 157-164. DOI:10.33545/26647222.2024.v6.i2b.136.
11. Ramya Teja Medarametla, D.J.S.K.; Dr. K Venkata Gopaiah.; SK Harshad.; P Nannessa.; P Ravishankar Durga Prasad.; P Mouli and R Lakshmi Pravallika., Utilization of artificial intelligence and computational modeling in nanomedicine., *Int. J. Pharm. Pharm. Sci.*, **2024**, 6(2), 106-109. DOI: 10.33545/26647222.2024.v6.i2b.130.
12. Sadybekov, A.V. and V. Katritch, Computational approaches streamlining drug discovery., *Nature.*, **2023**, 616(7958), 673-685. DOI: <https://doi.org/10.1038/s41586-023-05905-z>.
13. Fischer, A., Potential inhibitors for novel coronavirus protease identified by virtual screening of 606 million compounds., *International Journal of Molecular Sciences.*, **2020**, 21(10), 3626. DOI: <https://doi.org/10.3390/ijms21103626>.
14. Opo, F.A.D.M., Structure based pharmacophore modeling, virtual screening, molecular docking and ADMET approaches for identification of natural anti-cancer agents targeting XIAP protein., *Scientific reports.*, **2021**, 11(1), 4049. DOI: <https://doi.org/10.1038/s41598-021-83626>.
15. Yadav, M.R.; P.R. Murumkar, R. Yadav, and K. Joshi, Structure-based virtual screening in drug discovery, in *Cheminformatics., QSAR and Machine Learning Applications for Novel Drug Development.*, **2023**, Elsevier. 69-88.
16. Asiamah, I., Applications of molecular docking in natural products-based drug discovery., *Scientific African.*, **2023**, 20, e01593. DOI: 10.1016/j.sciaf.2023.e01593.
17. Muhammed, M.T. and E. Aki-Yalcin, Molecular docking: principles, advances, and its applications in drug discovery., *Letters in Drug Design & Discovery.*, **2024**, 21(3), 480-495. DOI: <https://doi.org/10.2174/1570180819666220922103109>.
18. Adelusi, T.I., Molecular modeling in drug discovery., *Informatics in Medicine Unlocked.*, **2022**, 29, 100880. DOI: <https://doi.org/10.1016/j.imu.2022.100880>.
19. Danel, T.; J. Ł ski.; S. Podlewska, and I.T. Podolak, Docking-based generative approaches in the search for new drug candidates., *Drug Discovery Today.*, **2023**, 28(2), 103439. DOI: <https://doi.org/10.1016/j.drudis.2022.103439>.
20. Netravati L. N, B.K.M.; Shilpa K. G. Bharathi S. V., Structural, Spectroscopic, Molecular Docking and Biological Evaluation of some novel Benzofuran Derivatives., *Orient J Chem.*, **2022**, 38(6), 1498-1504. DOI: <http://dx.doi.org/10.13005/ojc/380623>.
21. Othman L. A, M.S.R.; Ali M. K.; A Flexible Route to Synthesis and Molecular Docking of Some New Quinoline Derivatives through Imine and Cyclization Processes., *Orient J Chem.*, **2023**, 39(2), 356-363. DOI: <http://dx.doi.org/10.13005/ojc/390214>.
22. Arora P. K, K.S.; Bansal S. K.; Sharma P. C., Synthesis, *in-vitro* Cytotoxicity, Molecular Docking of Few Quinazolinone Incorporated Naphthyl Chalcones: As Potential Dual Targeting Anticancer Agents to Treat Lung Cancer and Colorectal Cancer., *Orient J Chem.*, **2023**, 39(2), 231-245. DOI: <http://dx.doi.org/10.13005/ojc/390202>.
23. Shaaban S.; A.-K.A.A.; Alhamzani A. R.; Abou-Krishna M. M, Al-Qudah M. A, Yousef T. A., Synthesis and Molecular Docking Analysis of New Thiazo-Isoindolinedione Hybrids as Potential Inhibitors of the SARS-Cov-2 Main Protease., *Orient J Chem.*, **2023**, 39(4), 913-918. DOI: <http://dx.doi.org/10.13005/ojc/390412>.
24. Saini P, K.S.; Characterization, Molecular Docking and Anti-Anxiety Evaluation of Some Novel Phenothiazine Derivatives., *Orient J Chem.*, **2023**, 39(5), 1232-1238. DOI: <http://dx.doi.org/10.13005/ojc/390516>.

25. Barot P. A, M.M.A.; Vora J. J., Exploring the Therapeutic Potential of Metal Complexes of Pregabalin and Terbutaline: Spectroscopic Insights and Molecular Docking in Alzheimer's and Parkinson's Disease., *Orient J Chem.*, **2024**, *40*(2), 459-469 DOI:http://dx.doi.org/10.13005/ojc/400219.
26. Dadhich I. A, P.N.B.; Dadhich K. A.; Dadhich C. S.; Exploring Benzimidazole Chemistry: Synthesis, Biological Activity, and Molecular Docking Studies for Alzheimer's Treatment., *Orient J Chem.*, **2024**, *40*(4), 1045-1055.DOI: http://dx.doi.org/10.13005/ojc/400415.
27. Fatiningtyas, F. A.; R. Napitupulu.; A. Malik, and I. Helianti, In Silico and In Vitro Inhibitory Activity of Indonesian Herbal Compound Extracts against SARS-COV-2 Recombinant Papain-Like Protease., *HAYATI Journal of Biosciences.*, **2025**, *32*(2), 356-366.DOI: https://doi.org/10.4308/hjb.32.2.356-366.
28. Ishikawa, T., *In Silico* Discovery of SARS-CoV-2 Main Protease Inhibitors Using Docking, Molecular Dynamics, and Fragment Molecular Orbital Calculations., *The Journal of Physical Chemistry B.*, **2025**.DOI: https://doi.org/10.1021/acs.jpcc.4c07920.
29. Cui, Z., Potential of umami molecules against SARS-CoV-2 (Omicron) S-RBD/hACE2 interaction: an *in-silico* study., *Journal of Future Foods.*, **2025**, *5*(3), 283-294.DOI: https://doi.org/10.1016/j.jfutfo.2024.07.008.
30. Hanson, Q., A High-Throughput Screening Pipeline to Identify Methyltransferase and Exonuclease Inhibitors of SARS-CoV-2 NSP14., *Biochemistry.*, **2025**.DOI: https://doi.org/10.1021/acs.biochem.4c00490.
31. Hu, Y., Single-and multiple-dose pharmacokinetics and safety of the SARS-CoV-2 3CL protease inhibitor RAY1216: a phase 1 study in healthy participants., *Antimicrobial Agents and Chemotherapy.*, **2025**, e01450-24.DOI:https://doi.org/10.1128/aac.01450-24.
32. Iacobucci, I., Cys44 of SARS-CoV-2 3CLpro affects its catalytic activity., *International Journal of Biological Macromolecules.*, **2025**, *295*, 139590.DOI:https://doi.org/10.1016/j.ijbiomac.2025.139590.
33. Flury, P., Design, Synthesis, and Unprecedented Interactions of Covalent Dipeptide-Based Inhibitors of SARS-CoV-2 Main Protease and Its Variants Displaying Potent Antiviral Activity., *Journal of Medicinal Chemistry.*, **2025**.DOI:https://doi.org/10.1021/acs.jmedchem.4c02254.
34. Yadav, T.; S. Kumar.; G. Mishra, and S.K. Saxena, Tracking the COVID-19 vaccines: The global landscape., *Human Vaccines & Immunotherapeutics.*, **2023**, *19*(1), 2191577.
35. Malhotra, M. and A.P. Singh, to evaluate the antiurolithiatic activity of aqueous extract of catharanthus roseus in ethylene-glycol-induced urolithiasis in rats., *International Journal of Current Pharmaceutical Research.*, **2024**, *16*(5), 27-31.DOI: 10.22159/ijcpr.2024v16i5.5027.
36. Malhotra, M.; H. Rana, and S. Tandon, exploring the therapeutic potential of catharanthus roseus: unveiling its diverse phytochemicals and mechanisms of action for chronic and infectious diseases., *International Journal of Current Pharmaceutical Research.*, **2024**, *16*(5), 1-8.DOI: 10.22159/ijcpr.2024v16i5.5023.
37. Ramadhiani, A.R.; U. Harahap, and A. Dalmunthe, nephroprotective activity of ethanol extract root of cogon grass (*imperata cylindrica* L. (Beauv.)) On creatinine, urea levels, and hematology profile against gentamycin-induced renal toxicity in rats., *Asian Journal of Pharmaceutical and Clinical Research.*, **2018**, *11*(13), 97-99. DOI: 10.22159/ajpcr.2018.v11s1.26578.
38. Kumari, I.; H. Kaurav, and G. Chaudhary, eclipta alba (bhringraj): a promising hepatoprotective and hair growth stimulating herb., *Asian Journal of Pharmaceutical and Clinical Research.*, **2021**, *14*(7), 16-23.DOI: 10.22159/ajpcr.2021.v14i7.41569.
39. Korassa, Y.B., Anti-alopecia activity of moringa (moringa oleifera lamk.) Seed oil against dihydrotestosterone-induced rabbits., *International Journal of Applied Pharmaceutics.*, **2023**, *15*(2), 19-24.DOI: 10.22159/ijap.2023.v15s2.04.
40. V Gnanambiga.; K.S., S Venkateswaran, PV Deepankumar.; RK Deepika and S Devilal., Preliminary phytochemical and Pharmacognostic study of Ipomoea quamoclit leave extract., *Int. J. Pharm. Pharm. Sci.*, **2022**, *4*(2), 01-06.DOI:10.33545/26647222.2022.v4.i1a.53.

41. M Sai Vishnu, T.P.S.; V Gunadeep Naidu, Asma Sulthana, MCK Phani Sai, K Bhumika, U Prakash, K Deepika and B Sravanthi Sai., Formulation and evaluation of paracetamol suspension by using natural suspending agent extracted from *Petalium murex* leaves., *Int. J. Pharm. Pharm. Sci.*, **2024**, 6(2), 19-26. DOI: 10.33545/26647222.2024.v6.i2a.120.
42. Rani., D.S.S.a.D.C.K., Qualitative phytochemical screening of *Acalypha indica* Linn., *Int. J. Pharm. Pharm. Sci.*, **2024**, 6(1), 124-126. DOI: 10.33545/26647222.2024.v6.i1b.110.
43. Velásquez, P.A., *Effectiveness of Drug Repurposing and Natural Products Against SARS-CoV-2: A Comprehensive Review. Clinical Pharmacology: Advances and Applications.*, **2024**, 1-25. DOI: <https://doi.org/10.2147/CPAA.S429064>.
44. Raman, K., Role of natural products towards the SARS-CoV-2: A Critical Review. *Annals of Medicine and Surgery.*, **2022**, 80, 104062. DOI: <https://doi.org/10.1016/j.amsu.2022.104062>.
45. Lobiuc, A., Future antimicrobials: Natural and functionalized phenolics., *Molecules.*, **2023**, 28(3), 1114. DOI: <https://doi.org/10.3390/molecules28031114>.
46. Newman, D.J. and G.M. Cragg, Natural products as sources of new drugs over the nearly four decades from 01/1981 to 09/2019., *Journal of Natural Products.*, **2020**, 83(3), 770-803. DOI: <https://doi.org/10.1021/acs.jnatprod.9b01285>.
47. Najmi, A.; S.A. Javed.; M. Al Bratty, and H.A. Alhazmi, Modern approaches in the discovery and development of plant-based natural products and their analogues as potential therapeutic agents., *Molecules.*, **2022**, 27(2), 349. DOI: <https://doi.org/10.3390/molecules27020349>.
48. Martin K. D. G.; P. K. G. V., Buan I. J. A., *In silico* Study of Ayapana Triplinervis Bioactive Compounds Against Quorum-Sensing System of *Pseudomonas Aeruginosa*., *Orient J Chem.*, **2021**, 37(1), 143-150. DOI: <http://dx.doi.org/10.13005/ojc/370119>.
49. Ramkumar R.; P.S.K., Molecular Docking Analysis for The Identification of Bioactive Compounds Against Urolithiasis (Hyperoxaluria)., *Orient J Chem.*, **2022**, 38(2), 336-342. DOI: <http://dx.doi.org/10.13005/ojc/380214>.
50. Tallur P. N, A.M.; Nayik V. M.; Bhat S. S., Pragasam A., Spectroscopic Identification of Isolated Bioactive Compounds from Methanolic Extract of *Psychotria dalzellii* leaves., *Orient J Chem.*, **2024**, 40(1), 300-306. DOI: <http://dx.doi.org/10.13005/ojc/400137>.
51. Kumar D, G.A.K.; Verma N.; Kumar S.; Extraction.; Isolation, Characterization and Nootropic Activity of Bioactive Compounds from Ethanolic Extract of Leaves of *Leucaena leucocephala*., *Orient J Chem.*, **2024**, 40(4), 1127-1133. DOI: <http://dx.doi.org/10.13005/ojc/400426>.
52. Satpal, D.; J. Kaur.; V. Bhadariya, and K. Sharma, *Actinidia deliciosa* (Kiwi fruit): A comprehensive review on the nutritional composition, health benefits, traditional utilization, and commercialization. *Journal of Food processing and Preservation.*, **2021**, 45(6), e15588. DOI: <https://doi.org/10.1111/jfpp.15588>.
53. Dwibedi, V., Inhibitory activities of grape bioactive compounds against enzymes linked with human diseases., *Applied microbiology and Biotechnology.*, **2022**, 106(4), 1399-1417. DOI: <https://doi.org/10.1007/s00253-022-11801-9>.
54. Zhou, D.-D., Bioactive compounds, health benefits and food applications of grape., *Foods.*, **2022**, 11(18), 2755. DOI: <https://doi.org/10.3390/foods11182755>.
55. Siddiqui, S. A.; S. Singh, and G.A. Nayik, Bioactive compounds from pomegranate peels-Biological properties, structure-function relationships, health benefits and food applications-A comprehensive review., *Journal of Functional Foods.*, **2024**, 116, 106132. DOI: <https://doi.org/10.1016/j.jff.2024.106132>.
56. Valero-Mendoza, A., The whole pomegranate (*Punica granatum. L*), biological properties and important findings: A review. *Food Chemistry Advances.*, **2023**, 2, 100153. DOI: <https://doi.org/10.1016/j.focha.2022.100153>.
57. Yang, X., The nutritional and bioactive components, potential health function and comprehensive utilization of pomegranate: a review., *Food Reviews International.*, **2023**, 39(9), 6420-6446. DOI: <https://doi.org/10.1080/87559129.2022.2110260>.

58. Gao, N., Polyphenol components in black chokeberry (*Aronia melanocarpa*) as clinically proven diseases control factors-An overview., *Food Science and Human Wellness.*, **2024**, 13(3), 1152-1167. DOI: <https://doi.org/10.26599/FSHW.2022.9250096>.
59. Popa, G.; D. Dragomir.; M. Dogaru, and a. Dobrin, Content of bioactive compounds and antioxidant activity in chokeberries juice (*aronia melanocarpa*)., *Scientific Papers. Series B. Horticulture.*, **2023**, 67(1).
60. Negreanu-Pirjol.; B.-S., Health benefits of antioxidant bioactive compounds in the fruits and leaves of *Lonicera caerulea* L. and *Aronia melanocarpa* (Michx.) Elliot., *Antioxidants.*, **2023**, 12(4), 951. DOI: <https://doi.org/10.3390/antiox12040951>.
61. Kondapuram, S.K.; S. Sarvagalla, and M.S. Coumar, Chapter 22 - Docking-Based Virtual Screening Using PyRx Tool: Autophagy Target Vps34 as a Case Study, in *Molecular Docking for Computer-Aided Drug Design*, M.S. Coumar, Editor. **2021**, Academic Press. p. 463-477.
62. Dallakyan, S. and A.J. Olson, Small-molecule library screening by docking with PyRx. *Chemical biology: methods and protocols*, **2015**, 243-250. DOI: [https://doi.org/10.1007/978-1-4939-2269-7\\_19](https://doi.org/10.1007/978-1-4939-2269-7_19).
63. Tian, W., CASTp 3.0: computed atlas of surface topography of proteins., *Nucleic Acids Research.*, **2018**, 46(W1), W363-W367. DOI: 10.1093/nar/gky473.
64. Shaker, B., User guide for the discovery of potential drugs via protein structure prediction and ligand docking simulation., *Journal of Microbiology.*, **2020**, 58, 235-244. DOI: <https://doi.org/10.1007/s12275-020-9563-z>.
65. Eberhardt, J.; D. Santos-Martins, A.F. Tillack, and S. Forli, AutoDock Vina 1.2.0: New Docking Methods, Expanded Force Field, and Python Bindings., *Journal of Chemical Information and Modeling.*, **2021**, 61(8), 3891-3898. DOI: 10.1021/acs.jcim.1c00203.
66. Trott, O. and A. J. Olson, AutoDock Vina: Improving the speed and accuracy of docking with a new scoring function, efficient optimization, and multithreading., *Journal of Computational Chemistry.*, **2010**, 31(2), 455-461. DOI: <https://doi.org/10.1002/jcc.21334>.
67. Huey, R.; G.M. Morris, and S. Forli, *Using AutoDock 4 and AutoDock vina with AutoDockTools: a tutorial*. The Scripps Research Institute Molecular Graphics Laboratory., **2012**. 10550(92037), 1000.
68. Zadorozhnyi, P.V.; V.V. Kiselev, and A.V. Kharchenko, *In silico* ADME profiling of salubrinol and its analogues., *Future Pharmacology.*, **2022**, 2(2), 160-197. DOI: <https://doi.org/10.3390/futurepharmacol2020013>.
69. Xiong, G., ADMETlab 2.0: an integrated online platform for accurate and comprehensive predictions of ADMET properties., *Nucleic Acids Research.*, **2021**, 49(W1): W5-W14. DOI: 10.1093/nar/gkab255.
70. Dong, J., ADMETlab: a platform for systematic ADMET evaluation based on a comprehensively collected ADMET database., *Journal of Cheminformatics.*, **2018**, 10(1), 29. DOI:10.1186/s13321-018-0283-x.
71. Yang, Y. and L. Du, SARS-CoV-2 spike protein: a key target for eliciting persistent neutralizing antibodies., *Signal transduction and targeted therapy.*, **2021**, 6(1), 95. DOI: <https://doi.org/10.1038/s41392-021-00523-5>.
72. Hussain, A., Targeting SARS-CoV2 spike protein receptor binding domain by therapeutic antibodies., *Biomedicine & Pharmacotherapy.*, **2020**, 130, 110559. DOI: <https://doi.org/10.1016/j.biopha.2020.110559>.
73. Luan, B., Targeting proteases for treating COVID-19., *Journal of Proteome Research.*, **2020**, 19(11), 4316-4326. DOI: <https://doi.org/10.1021/acs.jproteome.0c00430>.
74. Baby, K., *Targeting SARS-CoV-2 RNA-dependent RNA polymerase: An in silico drug repurposing for COVID-19*. F1000 Research., **2020**, 9. DOI: <https://doi.org/10.12688/f1000research.26359.1>.
75. Vicenti, I.; M. Zazzi, and F. Saladini, SARS-CoV-2 RNA-dependent RNA polymerase as a therapeutic target for COVID-19., *Expert Opinion on Therapeutic Patents.*, **2021**, 31(4), 325-337. DOI: <https://doi.org/10.1080/13543776.2021.1880568>.
76. Zhu, W., RNA-dependent RNA polymerase as a target for COVID-19 drug discovery. *SLAS discovery: Advancing the Science of Drug Discovery.*, **2020**, 25(10), 1141-1151. DOI: <https://doi.org/10.1177/2472555220942123>.

77. Shin, D., Papain-like protease regulates SARS-CoV-2 viral spread and innate immunity., *Nature*, **2020**, *587*(7835), 657-662. DOI: <https://doi.org/10.1038/s41586-020-2601-5>.
78. Capasso, C., A. Nocentini, and C.T. Supuran, Protease inhibitors targeting the main protease and papain-like protease of coronaviruses., *Expert opinion on therapeutic patents.*, **2021**, *31*(4), 309-324. DOI: <https://doi.org/10.1080/13543776.2021.1857726>.
79. Yuan, S., Targeting papain-like protease for broad-spectrum coronavirus inhibition., *Protein & Cell.*, **2022**, *13*(12), 940-953. DOI: <https://doi.org/10.1007/s13238-022-00909-3>.
80. Dyer, O., Covid-19: FDA expert panel recommends authorising molnupiravir but also voices concerns. *BMJ: British Medical Journal (Online).*, **2021**, *375*. DOI: [10.1136/bmj.n2984](https://doi.org/10.1136/bmj.n2984).
81. Lamb, Y.N.; Nirmatrelvir plus ritonavir: first approval., *Drugs.*, **2022**, *82*(5), 585-591. DOI: [doi.org/10.1007/s40265-022-01692-5](https://doi.org/10.1007/s40265-022-01692-5).
82. Dro d al, S., FDA approved drugs with pharmacotherapeutic potential for SARS-CoV-2 (COVID-19) therapy., *Drug Resistance Updates.*, **2020**, *53*, 100719. DOI: [doi.org/10.1016/j.drug.2020.100719](https://doi.org/10.1016/j.drug.2020.100719).
83. Walters, W.P., Going further than Lipinski's rule in drug design., *Expert Opinion on Drug Discovery.*, **2012**, *7*(2), 99-107. DOI: [10.1517/17460441.2012.648612](https://doi.org/10.1517/17460441.2012.648612).
84. Lagorce, D.; D. Douguet.; M.A. Miteva, and B.O. Villoutreix, Computational analysis of calculated physicochemical and ADMET properties of protein-protein interaction inhibitors., *Scientific Reports.*, **2017**, *7*(1), 46277. DOI: [10.1038/srep46277](https://doi.org/10.1038/srep46277).